

# THE AUTOMATIC EXTRACTION OF ROADS FROM LIDAR DATA

Simon CLODE<sup>a\*</sup>, Peter KOOTSOOKOS<sup>a</sup>, Franz ROTTENSTEINER<sup>b</sup>

<sup>a</sup> Intelligent Real-Time Imaging and Sensing Group,  
The University of Queensland, Brisbane, QLD 4072, AUSTRALIA  
sclode,kootsoop@itee.uq.edu.au

<sup>b</sup> School of Surveying and Spatial Information Systems,  
The University of New South Wales, Sydney, NSW 2052, AUSTRALIA  
f.rottensteiner@unsw.edu.au

Working Group III/3

**KEY WORDS:** Road, Detection, Extraction, LIDAR, DEM/DTM.

## ABSTRACT

A method for the automatic detection of roads from airborne laser scanner data is presented. Traditionally, intensity information has not been used in feature extraction from LIDAR data because the data is too noisy. This article deals with using as much of the recorded laser information as possible thus both height and intensity are used. To extract roads from a LIDAR point cloud, a hierarchical classification technique is used to classify the LIDAR points progressively into road or non-road. Initially, an accurate digital terrain model (DTM) model is created by using successive morphological openings with different structural element sizes. Individual laser points are checked for both a valid intensity range and height difference from the subsequent DTM. A series of filters are then passed over the road candidate image to improve the accuracy of the classification. The success rate of road detection and the level of detail of the resulting road image both depend on the resolution of the laser scanner data and the types of roads expected to be found. The presence of road-like features within the survey area such as private roads and car parks is discussed and methods to remove this information are entertained. All algorithms used are described and applied to an example urban test site.

## 1 INTRODUCTION

### 1.1 Motivation

Road extraction from remotely sensed data is a challenging issue and has been approached in many different ways by Photogrammetrists and digital image processors. Some of the methods are quite complex and require the fusion of several data sources or different scale space images. The goal of this paper is to suggest an extraction method that will provide results equivalent to other methods but relying solely on the acquired Light Detection And Ranging (LIDAR) data. Research on automated road extraction has been fuelled in recent years by the increasing use of geographic information systems (GIS), and the need for data acquisition and update for GIS (Hinz and Baumgartner, 2003). Existing road detection techniques, often require existing data and or semi-automatic techniques (Hager and Brenner, 2003) and produce quite poor detection rates.

This paper presents a simple and accurate method for the automatic detection of roads from LIDAR data or what is sometimes referred to as airborne laser scanner (ALS) data. Section 2 describes the background of road extraction including previous road detection methods from photogrammetry and satellite data. Section 3 describes how our new hierarchical classification technique is used to progressively classify the LIDAR points into a road image. The technique uses as much of the LIDAR information as possible, such as height and intensity. A full description of the steps involved is given and the algorithm is applied

to an actual urban data set. Results from the data set are discussed in Section 4 whilst conclusions and future work are examined in Section 5.

### 1.2 The Test Data

LIDAR data from Fairfield in Sydney, Australia, was initially collected with an approximate point density of 1 point per 1.3 m<sup>2</sup>.



Figure 1: The Fairfield Test Area.

The Fairfield data set is very interesting because of its diverse nature. Within the 2km x 2km area, the land usage

\*Corresponding Author.

changes quite dramatically. Fairfield is an urban area, however there are some rural-like parts with a heavily treed creek area running through the centre of the image. There are also both residential and industrial urban areas present. The industrial regions have larger buildings with many car parks and private roads whilst the residential regions have a much smaller average building and block size.

## 2 BACKGROUND

Road extraction from High-Resolution Airborne SAR data was performed in (Huber and Lang, 2001), by using operator fusion. A road was characterised by a central homogeneous region adjacent to two homogenous regions on either side of the road. A method for the automatic extraction of roads from multi-spectral satellite imagery is proposed by (Wiedermann and Hinz, 1999). The extraction strategy consists of finding the union of lines extracted from all available channels thus exploiting the nature of a multi-spectral sensor. A graph network is then constructed to derive the best paths and hence the road network itself.

The extraction of roads by varying the scale space of an image is another common approach. Extraction of roads from 1m-resolution satellite images was performed by (Lee et al., 2000), by varying the scale space and applying a watershed algorithm before knowledge extraction was performed based on gray levels and shape cues. Urban road networks are extracted from aerial imagery by (Hinz and Baumgartner, 2003). Scale-dependent models are explicitly formulated at both fine and coarse scales in order to extract both detailed and global information.

In (Heipke et al., 1997), three different road extraction techniques were evaluated. The LINE algorithm extraction is based on differential geometry, the TUM-G algorithm is based on the extraction of lines in an aerial image of reduced resolution using the approach of (Steger, 1996), and the extraction of edges in a higher resolution image. The TUM-S algorithm is similar to the TUM-G extraction except it uses "snakes" in the form of ribbon-snakes to the verify roads.

There have been several attempts to extract roads from LIDAR data but most require a form of data fusion to complete the task. In (Hatger and Brenner, 2003), LIDAR data is used in conjunction with existing database information to estimate the road geometry parameters. In (Rieger et al., 1999), roads were extracted from LIDAR data in forested areas. By detecting the road, breaklines could be generated and used to enhance the quality of the digital terrain model (DTM) produced. A combination of line and point feature extraction was then used to extract the final lines.

Traditionally, the intensity of the returned laser beam is registered by most LIDAR systems but this information has typically not been used for feature extraction. Unfortunately, given the footprint size (e.g. 20 - 30 cm) and an average point density of 1 to 2 metres the intensity image is under-sampled and very noisy (Rottensteiner et al., 2003,

Vosselman, 2002). In (Akel et al., 2003), the authors discuss a method for extracting a DTM in urban areas by initially estimating the DTM from the road network present.

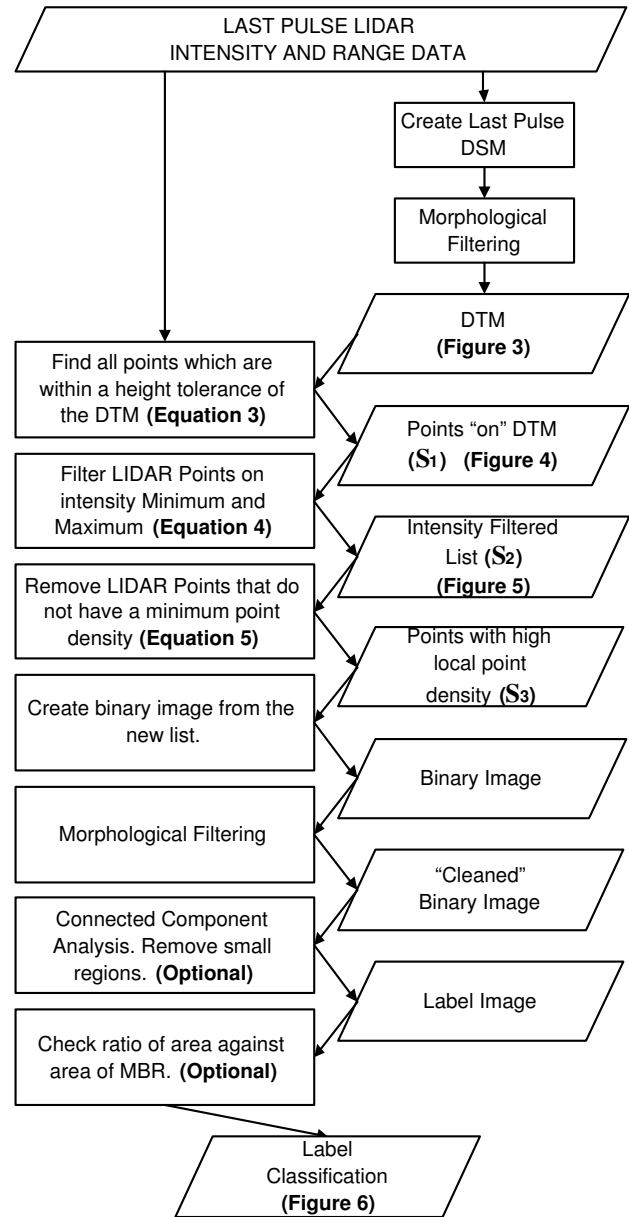


Figure 2: The Classification Work Flow.  $S_1$ ,  $S_2$  and  $S_3$  are explained in section 3.1.

Road models used by the previously mentioned authors are varied. (Heipke et al., 1997) bases his extractions on lines and road edges, (Huber and Lang, 2001) on homogenous regions and (Lee et al., 2000) on grey levels and shape cues.

The presented work flow algorithm detects a road model based on a continuous network of image pixels. Each road pixel has met a series of criteria, namely, LIDAR points lie on or near the DTM and have a certain intensity and normalised local point density. The image pixels appear as visible thick lines which form a road network containing all public roads. From the resultant image, existing image processing techniques can be used to extract information

such as centreline, edge and width.

The present paper limits the amount of data to only a subset of the original LIDAR points based on the intensity data, the closeness to the DTM, the LIDAR point density and the continuity of roads. By considering all of these criteria, it is possible to extract roads within a surveyed area effectively. By using the intensity and height information present in LIDAR data, a method is proposed for extracting roads from stand-alone LIDAR data.

### 3 EXTRACTING ROADS

#### 3.1 Classification Work-Flow

To extract roads from a LIDAR point cloud, a hierarchical classification technique is used to progressively classify the LIDAR points into road or non-road. The work-flow is described by Figure 2. For the purpose of this paper, we will describe any LIDAR data point  $\mathbf{p}_i$  as being defined by,

$$\mathbf{p}_i = (lp_x, lp_y, lp_z, lpi), \quad (1)$$

where  $lp_x$ ,  $lp_y$ , and  $lp_z$  represent the last pulse laser strike 3D coordinates and  $lpi$  represents the intensity of the last pulse strike. Let  $\mathbf{S}$  represent the set of all laser points collected, i.e.

$$\mathbf{S} = \{\mathbf{p}_1, \mathbf{p}_2, \dots, \mathbf{p}_N\}, \quad (2)$$

where  $\mathbf{p}_1, \mathbf{p}_2, \dots, \mathbf{p}_N$  are the individual LIDAR points.

As described in Figure 2, the first step in the hierarchical classification method is to sample the last pulse LIDAR data into a regular grid with minimal filtering to produce a last pulse digital surface model (DSM). A DTM is then created from the last pulse DSM by morphological grey scale opening using a square structural element. By progressively changing the size of the structural element and removing non-terrain type objects a DTM was obtained and displayed in Figure 3 (Rottensteiner et al., 2003).

By making the assumption that roads lie on or near the DTM, which is true except for elevated roads, bridges and tunnels, it is possible to disregard all LIDAR points that lie outside a given tolerance of the DTM (Akel et al., 2003). The creation of the subset is defined by (3).

$$\mathbf{S}_1 = \{\mathbf{p}_i \in \mathbf{S} : |\mathbf{p}_{i_{pz}} - \text{DTM}| < \Delta h_{\max}\}, \quad (3)$$

where  $\mathbf{p}_{i_{pz}}$  is the last pulse  $z$  coordinate of  $\mathbf{p}_i$ , DTM is the value of the smoothed DTM at location  $\mathbf{p}_i$  and  $\Delta h_{\max}$  is the maximum allowable difference between the  $\mathbf{p}_{i_{pz}}$  and the DTM.

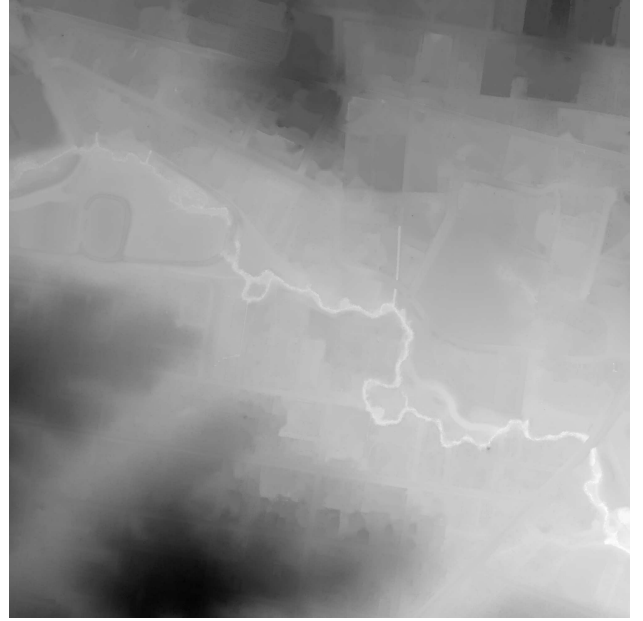


Figure 3: The Generated Fairfield DTM.

To help visualise the effect of the filtering, figure 4 displays an intermediate result showing the position of all existing points after applying (3). All non-terrain type objects (buildings and trees) have been removed and are displayed by areas of white whilst the strips of darker areas show areas of swath overlap, i.e. where there is a higher point density.

LIDAR points are then selected if their last pulse intensity values are between the acceptable range for the type of road material being detected (in this case bitumen). Even though the intensity values returned by the scanning unit are noisy, road material is typically uniform along a section of road. By searching for a particular intensity range it is possible to extract all LIDAR points that were on the road along with some other false positive (non-road) detections. If more than one type of road material is to be detected, two separate subsets should be obtained depending on the road material characteristics from (4). The union of the two resultant subsets should be taken to form the intensity filtered set  $\mathbf{S}_2$ . Equation 4 describes how the LIDAR points are filtered on their intensity to create a new subset of points

$$\mathbf{S}_2 = \{\mathbf{p}_i \in \mathbf{S}_1 : i_{\min} < \mathbf{p}_{i_{pi}} < i_{\max}\}, \quad (4)$$

where  $i_{\min}$  and  $i_{\max}$  are the minimum and maximum acceptable LIDAR intensities at point  $\mathbf{p}_i$ .

From the road model defined in Section 2, roads are depicted as a continuous network of pixels which form thick lines. Due to the nature of roads, a circle around an arbitrary road point  $\mathbf{p}$  will have at least a quarter of the circle lie on the road itself, provided the circles diameter is less than the road width. This is the worst case scenario and typically we would expect between a half and all the circle to lie on the road. By testing all points against a chosen



Figure 4: The points on the DTM.

minimum normalised local point density a new subset of points,  $S_3$ , is described as

$$S_3 = \{p_i \in S_2 : |\{p_j \in S_2 : \|p_i - p_j\|_2 < d\}| > \rho_{min}\}, \quad (5)$$

where  $d$  is the maximum distance from  $p_i$ , which can be any value less than or equal to half of the road width,  $\rho_{min}$  is the minimum normalised local point density required and  $\|p_i - p_j\|_2$  is the Euclidean distance from  $p_i$  to  $p_j$ .

An image is now created from the  $S_3$  subset. The image pixel size should loosely approximate the original average LIDAR point density. A binary image is created on an Is-Point/NotPoint basis. i.e. if there is a LIDAR point in subset  $S_3$  that lies within the pixel it is TRUE otherwise it is FALSE. A morphological closing with a small structural element of 3 pixels was performed to remove any small gaps in the road detection. Gaps can be caused by creating a smaller image pixel size than the original LIDAR point density or by single (isolated) reflections on vehicles and other objects on the road.

The resultant binary image now contains all public roads, private roads, car parks and some noise. The most obvious problem is car parks. Due to the industrial nature of the test data an attempt to remove some car parks was made. Unfortunately, it is very difficult to distinguish a car park from a road. Both are designed to have vehicle traffic thus have similar textures and properties. Some car parks (not all) are very wide and thus by defining a maximum acceptable road width prior to processing it is possible to remove larger car parks from the current binary image.

A label image is then created from the binary classification by connected component analysis. Labelled road regions



Figure 5: The road candidate points after intensity filtering.

that are very small in area are removed during the label image creation thus removing most of the noise present. These areas are assumed to be non-roads due to the continuous nature of road networks. The area of each individual label is checked against the area of its minimum bounding rectangle (MBR). As roads are a network of connected long thin objects the ratio of the two areas in the case of a diagonal road or road network will be very small. In the extreme case of detecting a single north-south or east-west road the ratio should not exceed a percentage based on the minimum side length of the MBR. For example, if the minimum side length of the MBR is 5 times the road width 20% would be the maximum threshold. Thus a threshold based on the ratio of areas is defined. Labels that do not meet this criterion are removed. As a morphological closing has been performed previously, the neighbouring patches of roads should now be connected into a continuous road structure. Figure 6 displays the final road classified image.

## 4 RESULTS

Figure 6 shows the resultant road detection from the suggested work flow. Ground truth data was obtained by manually digitising an orthophoto of the test area, (Figure 1) into road and non road areas. The guideline used during digitising was that public roads were to be classified as roads but car parks and private roads (driveways and roads leading to car parks) were not. The resultant ground truth image is shown in Figure 7. A visual comparison of the ground truth and binary classified data shows that there are still quite a number of car parks and small roads present. Road information such as centreline, edge and width can easily be obtained from the resultant classification by using existing image processing techniques. For example, the road centrelines have been detected using the phase coded

disk (PCD) approach discussed in (Clode et al., 2004). The centreline pixels have been displayed in Figure 8.

#### 4.1 Accuracy

The accuracy of any road extraction technique can be summarised by contemplating the completeness and correctness of the detected road network. In order to evaluate extraction results the quality measures completeness, correctness and quality as defined in (Heipke et al., 1997) are examined. For comparison purposes, the road extraction is classified as true positive (TP), false negative (FN) or false positive (FP) on a pixel by pixel basis.



Figure 6: The resultant work flow road network.



Figure 7: The public road ground truth model.

Completeness, sometimes called recall, is the ratio of the

correctly extracted records to the total number of relevant records within the ground truth data, as defined in (6),

$$\text{Completeness} = \frac{TP}{TP + FN}. \quad (6)$$

Correctness, sometimes called precision, is the ratio of the number of relevant records extracted to the total number of relevant and irrelevant records retrieved, as defined in (7),

$$\text{Correctness} = \frac{TP}{TP + FP}. \quad (7)$$

Quality is defined by

$$\text{Quality} = \frac{TP}{TP + FP + FN}. \quad (8)$$

Table 1 shows the results obtained from the work flow road extraction method when applied to the Fairfield test data.

	Completeness	Correctness	Quality
Work flow	0.86	0.69	0.62

Table 1: Work Flow Accuracy Results

Unfortunately, the work flow classification method can not be directly compared to other algorithms on the same area as data and information was not available. This makes a conclusive comparison difficult. In (Heipke et al., 1997) and (Wiedermann and Hinz, 1999) accuracy estimates were produced for the road extraction techniques used. Tables 2 and 3 show the results obtained from (Heipke et al., 1997) and (Wiedermann and Hinz, 1999) respectively.

From the published results it can be seen that the overall quality of the work flow is in the range of the better algorithm of (Heipke et al., 1997) and between the qualities achieved by (Wiedermann and Hinz, 1999). The difference in the quality figures for Site 1 and Site 2 of the algorithm from (Wiedermann and Hinz, 1999) illustrates the importance of comparing the extraction methods on the same test site before any conclusive comparison can be made. The correctness (and thus the quality) of the work flow classification method will improve in non-industrial areas.

	Completeness	Correctness	Quality
Lines	0.63	0.42	0.34
TUM-G	0.47	0.78	0.42
TUM-S	0.66	0.87	0.60

Table 2: Accuracy Results of Heipke et al. 1997

	Completeness	Correctness	Quality
Site 1	0.77	0.98	0.76
Site 2	0.61	0.94	0.59

Table 3: Accuracy Results of Weidemann and Hinz, 1999

As the extraction of the roads is partially based on the DTM generation of the surveyed area, elevated roads and

bridges can be a problem. This can be clearly seen in figure 9 which is an enlarged portion from the top left hand corner of figure 6. Passing horizontally through the middle of figure 9(a) is a row of trees delineating a creek. The road to be detected in the image runs approximately north-south. At the intersection of the road and the creek there is a bridge which has clearly not been detected in the binary classification image seen in figure 9(b).

## 5 CONCLUSION AND FUTURE WORK

### 5.1 Conclusion

This paper describes an effective and simple method for the detection of roads from LIDAR data using a hierarchical rule based system. The accuracy of the method has been shown to be on par with the better algorithms published. Results from this method can be expected to be equal to the quoted accuracies or better in non-industrial or commercial areas. The presence of many car parks and private roads has reduced the achieved correctness value due to the high presence of FP extractions.

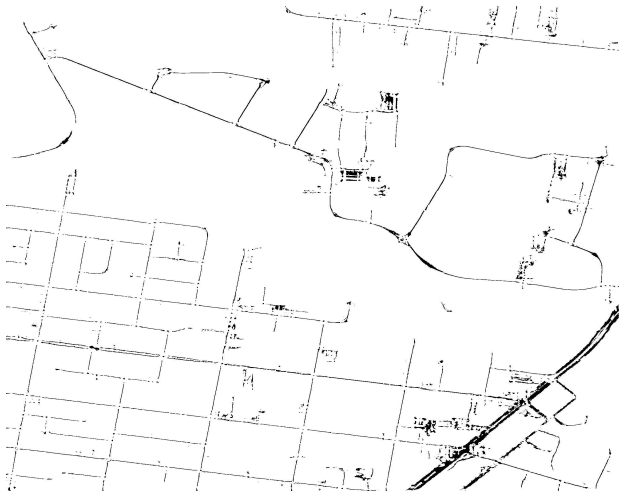


Figure 8: Centrelines.



(a) Bridge crossing the creek

(b) Missing road section.

Figure 9: Elevated road problem

### 5.2 Future Work

Improvements on the detection method are sought whilst the automatic extraction and vectorisation of the raw LIDAR data into approximate road straight, curve and spiral design primitives is a high priority.

## REFERENCES

- Akel, N. A., Zilberstein, O. and Doytsher, Y., 2003. Automatic DTM extraction from dense raw LIDAR data in urban areas. In: Proc. FIG Working Week <http://www.ddl.org/figtree/pub/> (accessed 20 Feb. 2004).
- Clode, S. P., Zelniker, E. E., Kootsookos, P. J. and Clarkson, I. V. L., 2004. A Phase Coded Disk Approach to Thick Curvilinear Line Detection. In: EUSIPCO.
- Hatger, C. and Brenner, C., 2003. Extraction of Road Geometry Parameters from Laser Scanning and Existing Databases. In: <http://www.isprs.org/commission3/wg3/> (accessed 20 Feb. 2004).
- Heipke, C., Mayer, H., Wiedemann, C. and Jamet, O., 1997. Evaluation of Automatic Road Extraction. In: IAPRS, Vol. 32, pp. 47–56.
- Hinz, S. and Baumgartner, A., 2003. Automatic Extraction of Urban Road Networks from Multi-View Aerial Imagery. ISPRS Journal of Photogrammetry and Remote Sensing 58/1-2, pp. 83–98.
- Huber, R. and Lang, K., 2001. Road Extraction from High-Resolution Airborne SAR using Operator Fusion. In: Proc. International Geoscience and Remote Sensing Symposium <http://www.cosy.sbg.ac.at/reini/reini.html> (accessed 20 Feb. 2004).
- Lee, H. Y., Park, W., Lee, H.-K. and Kim, T.-G., 2000. Towards Knowledge-Based Extraction of Roads from Im-resolution Satellite Images. In: Proc. IEEE Southwest Symposium on Image Analysis and Interpretation, Austin, U.S.A, pp. 171–176.
- Rieger, W., Kerschner, M., Reiter, T. and Rottensteiner, F., 1999. Roads and Buildings from Laser Scanner Data within a Forest Enterprise. In: IAPRS, ISPRS Workshop, Vol. 32, La Jolla, California, pp. 185 – 191.
- Rottensteiner, F., Trinder, J., Clode, S. and Kubic, K., 2003. Building detection using LIDAR data and multi-spectral images. In: Proceedings of DICTA, Sydney, Australia, pp. 673–682.
- Steger, C., 1996. Extracting Curvilinear Structures: A Differential Geometric Approach. In: Proc. Fourth European Conference on Computer Vision, Vol. 1064, pp. 630–641.
- Vosselman, G., 2002. On the Estimation of Planimetric Offsets in Laser Altimetry Data. In: IAPRSIS, Vol. XXXIV/3A, pp. 375–380.
- Wiedemann, C. and Hinz, S., 1999. Automatic Extraction and Evaluation of Road Networks from Satellite Imagery. In: IAPRS, Vol. 32, pp. 95–100.

## ACKNOWLEDGEMENTS

This research was funded by the ARC Linkage Project LP0230563 and the ARC Discovery Project DP0344678. The Fairfield data set was provided by AAMHatch, Queensland, Australia. (<http://www.aamhatch.com.au>)